eMagRes
MRI | NMR

Phosphorus Spectroscopy (^{31}P MRS) of the Brain in Psychiatric Disorders

David G. Harper[1,2], J. Eric Jensen[1,2] & Perry F. Renshaw[3]

[1] *McLean Hospital, Belmont, MA, USA*
[2] *Harvard Medical School, Boston, MA, USA*
[3] *University of Utah, Salt Lake City, UT, USA*

Some of the most important biological molecules responsible for the maintenance of cellular homeostasis, high-energy phosphates and phospholipids, are amenable to quantification using spectroscopy targeted at the phosphorus 31 isotope (^{31}P MRS). For example, the brain, while typically comprising 2% of the body's mass, uses 20% of its energy, and quantification of bioenergetic molecules can provide important information about cellular energy usage and storage. In addition, phospholipids, which form the basis of cellular membrane bilayers not only segregate organelles from the cellular environment and cells from the interstitial environment but are also critical in providing important second messenger signaling. The activity of these phosphorus compounds has been demonstrated to be altered in psychiatric disorders. Cellular energy utilization is demonstrably altered in mood disorders, and phospholipid metabolism is different in patients with schizophrenia when compared to normal control populations. There are challenges and complexities associated with implementing ^{31}P MRS, and difficulties with detection efficiency, spatial localization, and spectral quantification present challenges to the study of psychiatric disorders. Much work remains to be done in interpreting the observed bioenergetic and cell membrane changes in disease states, but continued progress in methodology and experimental design should allow for a deeper understanding of the relationship between alterations in phosphorus compounds and psychiatric disorders.

Keywords: depression, bipolar disorder, schizophrenia, adenosine triphosphate, phosphocreatine, inorganic phosphate, creatine kinase, phospholipids, phospholipase A2, arachidonic acid

How to cite this article:
eMagRes, 2016, Vol 5: 1257 – 1270. DOI 10.1002/9780470034590.emrstm1463

Introduction

Phosphorus magnetic resonance spectroscopy (^{31}P MRS) is a useful and noninvasive probe allowing in vivo and in vitro examination of phosphorus-containing compounds in the brain. These compounds are some of the most important molecules in cellular physiology, being essential for maintaining homeostatic equilibrium and facilitating cellular survival. Usable cellular energy is stored in the form of high-energy phosphates that are attached to an adenosine molecule. These adenosine triphosphate (ATP) molecules act as units of cellular energy that are ready for utilization in the cell. Since ATP is the prime source of energy needed by the cell to function, its production and concentration must be kept in balance. Phospholipids, on the other hand, are the main constituents of cellular membranes, which form a bilayer with polar phospholipid head groups facing the aqueous internal and external environments of the cell, and the nonpolar tails facing inward to create a hydrophobic boundary layer through which water molecules and water-soluble compounds cannot pass unaided. Membrane turnover in the cell involves the continuous breakdown and recombining of these phospholipids to maintain membrane integrity. In addition, metabolism of phospholipids is a major source of hydrophobic second messengers (e.g., arachidonic acid) that are involved in inflammation and other cellular activities. ^{31}P MRS, which detects signals from ATP and some of its associated metabolites and also from phospholipid molecules, can therefore provide unique information on cellular energy utilization as well as several important membrane phospholipid precursors and metabolites involved in cell membrane turnover and second messenger systems.

Cellular Energetics

ATP in the brain can be generated from adenosine diphosphate (ADP) and inorganic phosphate (Pi) by three mechanisms. Firstly, ATP is generated in mitochondria by the action of ATP synthase on the substrates ADP and Pi via oxidative phosphorylation. Energy for the reaction is derived from a proton gradient that exists across the inner mitochondrial membrane, induced by the electron transport chain and, the metabolism of glucose. The overall reaction can be summarized as follows:

$$\mathrm{ADP} + \mathrm{Pi} \Longleftrightarrow \mathrm{ATP} \qquad (1)$$

The energy stored in the 'high-energy' phosphate bond of ATP is utilized throughout the body. In the central nervous system (CNS) it is used for the transport of ions and metabolites across membranes by coupled reverse reactions catalyzed by ATPases, which transform ATP to Pi and ADP. Pi, in addition to being a metabolic byproduct of ATP utilization, also serves the

regulatory function of promoting oxidative phosphorylation as the concentration of Pi builds from metabolic activity.

Secondly, a reservoir of 'high-energy' phosphate is also maintained in a ready-to-use state throughout the cytoplasm through the action of phosphocreatine (PCr) and the creatine kinase (CK) enzyme. The CK transfers a high-energy phosphate from PCr to ADP by maintaining the following equilibrium.

$$PCr + ADP + H^+ \Longleftrightarrow ATP + Cr^- \qquad (2)$$

PCr can be considered a 'high-energy' phosphate buffer that can quickly replete the supply of ATP from ADP at sites distal to the mitochondria. Finally, ATP can be generated inefficiently but quickly by anaerobic glycolysis. Compared to oxidative phosphorylation, which produces 26 molecules of ATP/molecule of glucose, glycolysis produces 2 molecules of ATP/molecule of glucose.

Cellular Membranes

Biological membranes serve numerous essential cellular functions and their constituents are phosphorus-rich compounds whose anabolic precursors (phosphomonoesters, PME) and catabolic products (phosphodiesters, PDE) are amenable to examination with ^{31}P MRS even at the (now) relatively low field strength of 1.5 T. Phosphatidylcholine and phosphatidylethanolamine are the two most prevalent membrane phospholipids, each comprising approximately 45% of the CNS total membrane phospholipid pool.[1] Measuring the PME precursors and PDE metabolites of these two important membrane phospholipids can give insight into the state of membrane integrity and turnover.[2,3] The ^{31}P MRS components of PME that can be resolved into independent peaks at 4 T field strength or by using proton (^{1}H)-decoupling techniques are phosphocholine (PCho) and phosphoethanolamine (PEtn). The PDE peaks that can be resolved at 4 T are glycerophosphocholine (GPCho) and glycerophosphoethanolamine (GPEtn). Examination of these two peaks can give insight into the state of membrane integrity and turnover.[2,3]

Basic Brain ^{31}P MRS

Brain ^{31}P MRS has special challenges compared to brain ^{1}H MRS. Here, a brief review of the properties and limitations of the method are provided as a context for the review of the clinical studies that follow.

The In Vivo Phosphorus Brain Spectrum

The in vivo ^{31}P MRS spectrum from the brain is comprised of NMR-visible resonances that span a chemical shift range of about 23 ppm (Figure 1). The largest and main spectral resonance peak arises from PCr, which is a singlet referenced to 0.0 ppm. The other main resonance structure originates from ATP and is comprised of three peaks located at 2.5 ppm (γ-ATP), 7.5 ppm (α-ATP), and 16.0 ppm (β-ATP) downfield from PCr. Since ATP is J-coupled it appears as two doublet peaks (γ- and α-ATP) and one triplet peak (β-ATP). Inorganic phosphate (Pi) is also a singlet peak at 4.85 ppm upfield from PCr, in the healthy brain, but its chemical shift can vary with

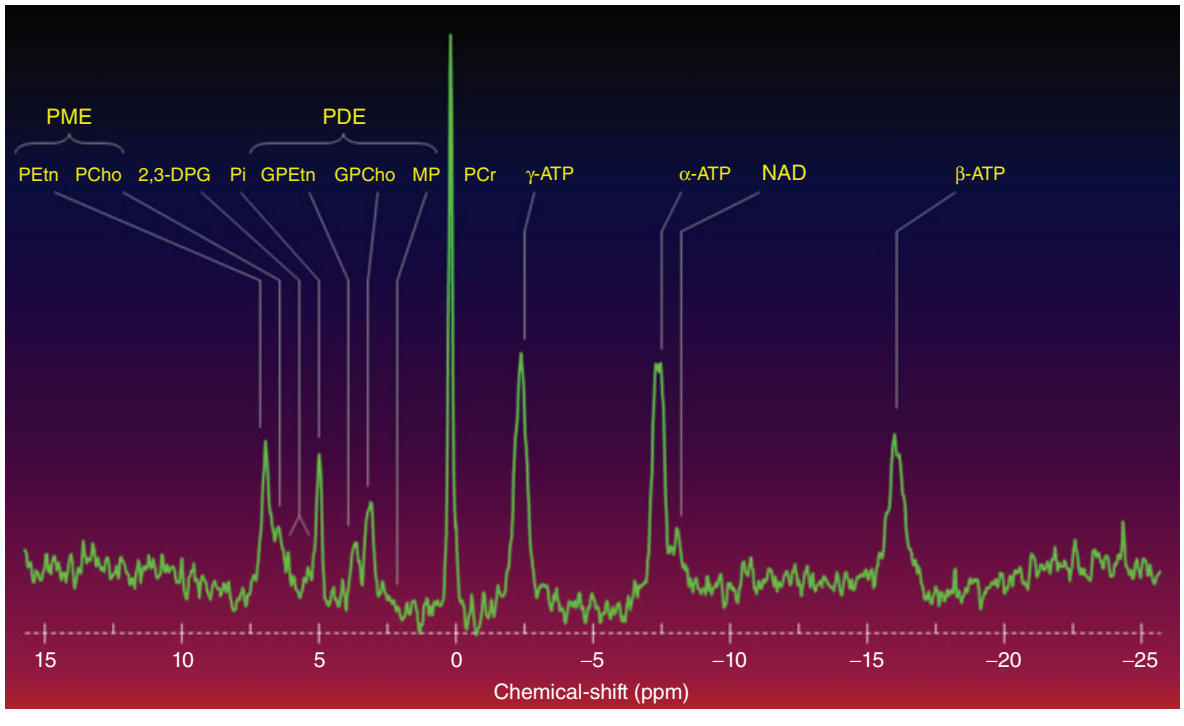

Figure 1. In vivo brain ^{31}P spectrum from a human at 4 T field strength. PME, phosphomonoesters; PDE, phsophodiesters; PEtn, phosphoethanolamine; PCho, phosphocholine; 2,3 DPG, diphosphoglycerate; Pi, inorganic-phosphate; GPEtn, glycerophosphoethanolamine; GPCho, glycerphosphocholine; MP, membrane-bound phospholipids; PCr, phosphocreatine; γ-, α-, β-ATP-adenosine triphosphate; NAD, dinucleotides

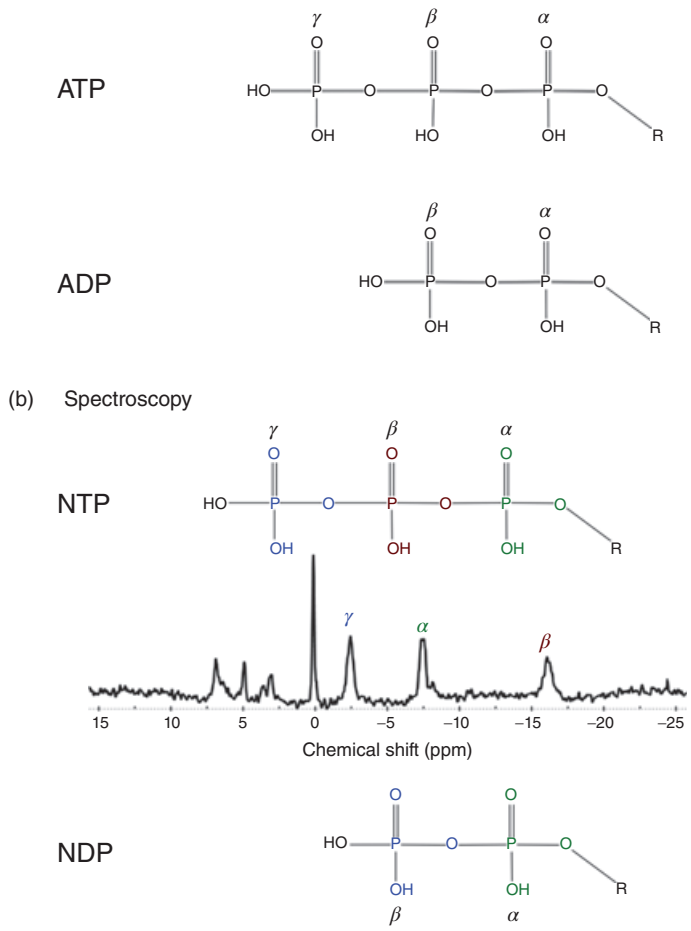

Figure 2. Phosphate labeling on the adenosine triphosphate (ATP) and adenosine diphosphate (ADP) molecules. (a) The biochemical convention is to label the phosphates α, β, and γ starting at the adenosine group (R) for both ATP and ADP. (b) In MRS, the chemical shift of the β-phosphate of ADP coincides with the α-phosphate resonance of ATP. This means that only the β-phosphate resonance is unique to NTP. In addition, there are small contributions from the phosphates of purine and pyrimidine (R) molecules other than adenosine (cytidine, guanosine, uridine), which fall at the same chemical shifts as the α-, β-, and γ-phosphates of ATP (green, red, and blue labels, respectively). Therefore, it is prudent to label the triphosphate resonances as deriving from nucleoside triphosphate (NTP) and the diphosphate contributions as NDP (green and blue labels on the α- and β-phosphates, respectively)

intracellular pH (see below). Note that the peaks assigned to γ-ATP and α-ATP also contain small contributions (typically <0.1 mM) from the β- and α-phosphates of ADP, respectively. The difference in the labeling of these phosphate groups arises from the labeling convention of starting at the adenosine moiety (R), so that the γ-phosphate is outermost on ATP while the β-phosphate is outermost on ADP and these two peaks occur at very similar chemical shifts (Figure 2). Because β-ADP overlaps and is much smaller than γ-ATP, the distinction is often lost. In addition, the quantification of the ATP peaks will also include high-energy triphosphates of purine or pyrimidine (R) molecules other than adenosine (cytidine, guanosine, uridine). Therefore, the triphosphate resonances are often more appropriately referred to as deriving from *nucleoside* triphosphate (NTP), although the other contributions are, again, small.

The phospholipid resonances are considerably more complex due to J-coupling and overlapping resonance lines. At 4 T, these compounds appear much smaller compared to PCr and NTP, making their quantification more challenging. The individual PME constituents involved in phospholipid membrane synthesis are primarily free floating in the cytosol: they have resonances composed of PEtn (6.85 ppm), phsophatidylserine (PSer; 6.52 ppm), and PCho (6.25 ppm). The free-floating constituents resulting from the metabolism of phospholipid membranes – PDE – are also upfield from PCr and are modeled as a single peak at lower field strengths where they appear as a much broader but more intense peak. At higher field strengths (4 T) GPEtn (3.54 ppm) and GPCho (2.97 ppm) are modeled as individual spectral resonances. They are, however, weakly J-coupled groupings. A broad underlying resonance component exists at 2.25 ppm upfield from PCr and originates primarily from rigidly membrane-bound phospholipid components with little motional mobility. A small resonance exists just downfield from γ-NTP and is actually a small and tight grouping of individual peaks arising mostly from phosphorylated dinucleotides (NAD/NADPH 8.35 ppm) involved in electron transport.

^{31}P MRS Detection Efficiency

Several inherent properties of the ^{31}P nucleus impact the efficiency and clinical utility of ^{31}P MRS. First, the ^{31}P MRS signal is noisy owing to the inherently low sensitivity of the ^{31}P nucleus, which is 1/16th that of the hydrogen (^{1}H-proton) nucleus. This means that longer MRS signal averaging times and the interrogation of larger tissue voxel volumes are required to compensate for the low signal-to-noise ratio (SNR) of the ^{31}P MRS signal. Second, other than PCr, the phosphorus-containing molecules have relatively short spin–spin relaxation times (T2), which means that the ^{31}P MRS signal decays to baseline noise levels faster than many ^{1}H metabolites. Low T2 is detrimental to ^{31}P MRS since it reduces spectral resolution (the ability to separate and quantify overlapping resonances) and SNR. Third, phosphorus-containing molecules tend to have long spin–lattice relaxation times (T1), hence the ^{31}P MRS signal takes longer to recover from the repeated excitations needed for signal averaging, which further reduces detection efficiency. This property also directly reduces the SNR and introduces a T1 bias into the spectrum when short repetition periods (TR) are used. These properties of ^{31}P all reduce the SNR, which, when coupled with the millimolar level concentrations of phosphorus-containing molecules in the brain, render ^{31}P MRS a physically challenging yet biochemically information-rich noninvasive analytical technique.

Spatial Localization

The real power and clinical utility of ^{31}P MRS arises in its ability to localize and isolate signals from anatomically specific regions in the brain. Many clever techniques have been devised through the years to improve the degree of localization and signal quality of ^{31}P MRS. One of the earliest techniques to isolate ^{31}P spectral signal from cortical gray matter (GM) used a simple surface RF coil placed on the scalp and spatially selective excitation to minimize the contaminating ^{31}P signal from subcutaneous muscle. This technique, known as *DRESS* (*depth-resolved spectroscopy*; see ***Single-Voxel MR Spectroscopy***), is effective for cortical ^{31}P MRS, but cannot access the deeper brain structures such as the basal ganglia and thalamic regions.

An alternative method that allows for the simultaneous acquisition of multiple voxels throughout the brain is MRSI (magnetic resonance spectroscopic imaging; see ***CSI and SENSE CSI***). MRSI uses a sequence of pulsed phase-encoding magnetic field gradients to acquire a matrix of spatially resolved ^{31}P spectra in either two or three dimensions throughout the brain. Depending on the degree of coverage desired, as well as scan-time considerations, spatially resolved ^{31}P spectra can be acquired over a two-dimensional slab with the addition of a manually prescribed frequency-selective pulse or acquired from a three-dimensional matrix by phase encoding in all three dimensions. This technique is efficient but requires a whole-head RF coil in order to access the deeper tissue, with the added complexity of having to operate the scanner at both the ^{1}H and ^{31}P frequencies if the ^{31}P spectral data are to be coregistered with the anatomy or pathology as visualized by ^{1}H MRI. MRSI can also accommodate post-acquisition repositioning of voxels over anatomical regions of interest. This is accomplished as a result of the phase-encoding nature of MRSI wherein the entire 2-D or 3-D grid of voxels can be shifted in space relative to the MRI, to fine-tune voxel position by phase shifting the FT reconstruction.

The multivoxel advantage of MRSI can also benefit from tissue segmentation of GM, white matter (WM), and cerebrospinal fluid (CSF) based on coregistered MRI scans. Voxel segmentation refers to the mathematical quantification of the relative amounts of each tissue type within each voxel using specialized software and high-resolution reference MRIs. This analysis yields both ^{31}P spectral and anatomical data that are specific for each voxel. Statistically, this can be a very powerful technique that takes advantage of the multiple voxels and statistical regression of ^{31}P spectral data as a function of tissue type to isolate the different ^{31}P biochemical characteristics of the various tissue compartments.

Spectral Quantification

Much effort has been focused on quantifying each phosphorus-containing biomolecule in the ^{31}P spectrum. This is because the molecular concentration of a given compound is proportional to the integrated area under the spectral peak. The peak areas can be determined by direct processing of the spectrum itself – referred to as frequency-domain processing; or processing in the time-domain – which involves mathematical modeling of the raw FID signal to derive peak areas. Modeling in either domain typically utilizes prior spectral knowledge including line shapes, J-coupling constants, peak phases, and chemical shifts (Figure 3), and can involve iterative and nonlinear fitting to converge on a 'best-fit' result that minimizes the difference between the model spectrum and the raw time- or frequency-domain data. Details of these techniques are found elsewhere (see ***Quantifying Spectra in the Frequency Domain***; ***Advanced Spectral Quantification: Parameter Handling, Nonparametric Pattern Modeling, and Multidimensional Fitting***; ***Time-Domain Methods for Quantifying MR Spectra***). Special challenges for in vivo ^{31}P quantification of individual concentrations are the inherently low SNR, overlap of the phospholipid resonances, and spectral baseline roll arising from rigidly bound membrane phospholipids and bone.

The derivation of millimolar (mM) concentrations requires an internal or an external concentration reference whose peak area is also measured. As detailed in ***Quantifying Metabolite Ratios and Concentrations by Non-^{1}H MRS***, the ratio of the metabolite peak area to that of the reference is then multiplied by a number of correction factors to yield the metabolite concentrations. The corrections typically involve (i) relaxation corrections based on published values of NMR T1 and T2 values; (ii) assumed biological reference concentrations such as that of endogenous ATP or water content; and (iii) direct measurements, such as tissue partial volume fractions in each voxel (to account for potentially differing metabolite concentrations in GM, WM, and CSF), receiver gain, RF coil sensitivity, and so on. However, to date, many ^{31}P MRS studies of the human brain have expressed metabolite values as simple ratios to the total integrated phosphorus signal, that is, the summed area under all of the NMR-visible peaks. The use of simple ratios in arbitrary units of the metabolite of interest compared to

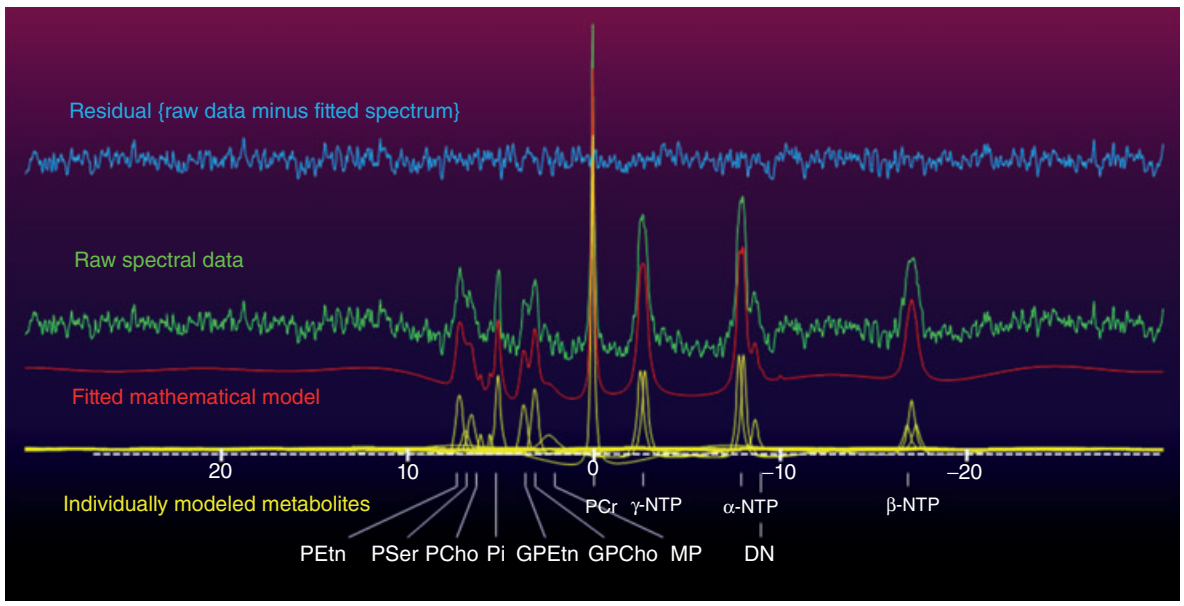

Figure 3. In vivo brain ^{31}P spectrum from 4 T depicting the raw data (green), the fitted spectral model (red), the individually modeled spectral components (yellow), and the optimized residual signal (blue)

the total signal is also referred to as the mole percent of the metabolite.

Brain tissue concentrations of ATP derived from chemical analysis of brain tissue have been found to be remarkably stable and in a range varying from 2.30 to 3.10 μmol g^{-1} wet weight whereas ADP has been observed to be much lower and in the range of 0.21–0.56 μmol g^{-1}.[4] Therefore, a trade-off exists between the use of the γ- and the β-phosphate signal of NTP to estimate the level of ATP. The γ-phosphate signal has in its favor its proximity to PCr in experimental configurations where transmit and receive bandwidths are limited, but the inclusion of ADP in the measurement means the peak does not purely measure NTP. The β-phosphate does not have any ADP but may be attenuated by off-resonance effects due to its ∼16 ppm offset from PCr. Another option is to sum the three nucleoside components (i.e., the α-, β-, and γ-signals) to provide an index of the 'total integrated NTP'.

The quantification of PCr and Pi is less problematic. Brain levels of these two metabolites have been measured chemically to be in the range of 4.0–5.5 and 2.2–2.8 μmol g^{-1} respectively.[4] As noted earlier, PCr serves as a 'ready reserve' of high-energy phosphate to replete ATP from ADP, thereby storing energy for release as needed. In this way PCr acts as a *temporal* buffer of high-energy phosphate transferring high-energy phosphate to ADP to form ATP at average rates of about 30 $\mu mol^{-1}\ s^{-1}\ g^{-1}$ versus the 2.5 $\mu mol^{-1}\ s^{-1}\ g^{-1}$ for oxidative phosphorylation.[5] PCr may also serve as a *spatial* buffer for transferring high-energy phosphate molecules from the site of oxidative phosphorylation in the mitochondria to ADP molecules located in the cytoplasm[6,7] in organs with high energy requirements such as the brain.

Pi is believed to serve as a metabolic control on mitochondrial oxidative phosphorylation[8] acting as a substrate at the site of ATP synthase, and at several other sites involved with metabolic control. These mechanisms include controlling levels of reduced nicotinamide adenine dinucleotide, [NADH], and NADH-generating capacity, influencing the matrix pH, membrane potential, oxygen consumption, and cytochrome reduction level.[9] Pi has been found to regulate succinyl CoA-synthetase[10] and to be an active regulator of complex III.[11] This regulation suggests that there should be a dynamic balance between the levels of Pi and molecules containing high-energy phosphates such as ATP and PCr. Any breakdown in this relationship could signal significant problems in the energetic homeostasis of the cell.

Aside from the direct estimation of the individual concentrations of the phosphorus-containing molecules, ^{31}P MRS also allows for the determination of the hydrogen ion concentration or pH, which is another important biomarker that measures the degree of acidosis in metabolically compromised tissue, for example. The pH value is determined by measuring the chemical shift difference between the PCr and Pi resonances. Chemical shift difference is used to calculate the pH value,[12] which is approximately 7.2–7.4 in the healthy human brain tissue, decreasing with acidotic conditions such as in acute ischemia or hypoxia. Another quantity that can be indirectly assessed using ^{31}P MRS is the magnesium ion concentration, $[Mg^{2+}]$, or pMg in the brain. Similarly to pH, $[Mg^{2+}]$ can be calculated by measuring the chemical shift separation of the PCr and β-ATP resonances, using a semiempirical equation.[13] These measurements are useful because intracellular Mg^{2+} is coupled to ATP production. Along with hydrogen ions, Mg^{2+} is an important cofactor in the CK reaction, which affects the rate of rephosphorylation of ATP from ADP[14]: lower pH (with consequent higher $[H^+]$) and lower pMg (with consequent higher Mg^{++}) are associated with higher rates of rephosphorylation of ATP. In the healthy human brain, $[Mg^{2+}]$ is approximately 0.3 mM.

A more advanced ^{31}P MRS technique, known as *magnetization transfer* (*MT*), allows for the assessment of reaction rates associated in the phosphate exchange of the CK reaction, which governs the rate of ATP production in the cell from PCr. MT is accomplished through selective irradiation of the γ-ATP resonance during ^{31}P MRS acquisition, which affects the magnitude of the PCr resonances. The forward reaction rate, k_1 or k_{for}, can then be calculated through the measurement of these magnitude changes. This technique is detailed in ***Measuring Biochemical Reaction Rates In Vivo with Magnetization Transfer***.

^{31}P MRS Studies of Energetics in Psychiatric Illness

Unipolar Depression

A summary of results from bioenergetic studies of depression is presented in Table 1. Early ^{31}P MRS studies quantified decreases in NTP in the basal ganglia[16,18] and in the dorsolateral prefrontal cortex[17] of patients with major depressive disorder (MDD).[21] Reductions in PCr in frontal regions have also been observed in severe, as compared to mild, depression[15] in cohorts of mixed unipolar and bipolar subjects. However, even though basal ganglia β-NTP has been observed to be lower in major depression when compared to controls, the association with depressive symptoms within the group of patients with depression has been the opposite of what would be expected with increased depressive symptoms, as measured by the Hamilton Depression Rating Scale (HAMD),[22] associated with higher β-NTP within the group of patients with depression.[18] However, in the same study, lower β-NTP in the basal ganglia was found to be associated with a likelihood of response to antidepressant treatments in MDD.

A more recent study of major depression using a higher field strength (4 T) and a larger slice centered on the anterior cingulate cortex[19] did not show any differences in energetic metabolites in a population of patients with major depression who were resistant to treatment with selective serotonin reuptake inhibitor (SSRI) antidepressants and who were on medication at the time of the MRS study. Augmentation treatment with tri-iodothyronine caused, in treatment responders only, a significant elevation in total NTP and a concomitant decrease in PCr, suggesting that energetic normalization could be associated with a resolution of depressive symptoms in a subgroup of patients.

Another study conducted at 4 T employing three-dimensional MRSI[20] observed a highly significant reduction in β-NTP and total NTP in a cohort of patients with late-life depression when compared to controls. However, this reduction in total NTP could be entirely explained by differences between the groups in WM but not GM. Sertraline treatment did not significantly change the levels of these metabolites from their baseline levels.

Bipolar Disorder

A summary of results from ^{31}P MRS studies of bioenergetics in bipolar disorder is presented in Table 2. The early studies of bipolar disorder were performed using surface coils. In patients diagnosed with bipolar disorder, the earliest finding was a reduction in pH (or increased $[H^+]$) in the euthymic state when compared to controls.[23] This was only true for patients diagnosed with bipolar disorder type I,[21] whereas in patients with type II bipolar disorder pH was not significantly different from that in normal controls.[24] This finding was later confirmed in voxels localized to the basal ganglia and also over the whole brain.[27] PCr has also been seen to be reduced in the frontal cortex when observed with a surface coil.[24] This effect was found to be lateralized to the left in a further study with voxels placed bilaterally in the frontal cortex.[31]

In the above studies, patients were generally taking medication to control their bipolar disorder. In studies conducted with unmedicated men with bipolar disorder[25] and another focusing on adolescents,[28] a portion of whom were also unmedicated, no pH differences were observed. Medication status also appears

Table 1. Unipolar depression and bioenergetics

References	Sample size	Age	Sex	Medication status	Target	Metabolite
Kato *et al.*[15]	11 mild depression 11 severe depression	<60	Unknown	Unknown	Frontal lobe (DRESS)	↓ PCr in severe depression
Moore *et al.*[16]	35 MDD 18 control	37.2 ± 8.5 38.2 ± 9.9	16M : 19F 9M : 9F	Unmedicated	Basal ganglia	↓ β-NTP in MDD Group
Volz *et al.*[17]	14 MDD 8 control	43.8 ± 12.5 41.5 ± 13.7	6M : 8F 3M : 5F	11 medicated	Bilateral frontal lobe	↓ β-NTP in MDD Group
Renshaw *et al.*[18]	12 MDD 17 control	38.9 ± 10.1 39.9 ± 9.7	Unknown	Unmedicated	Left basal ganglia	↓ β-NTP in MDD Group
Iosifescu *et al.*[19]	19 MDD 9 control	43.6 ± 10.0 40.0 ± 10.1	8M : 11F 4M : 5F	19 medicated	Anterior cingulate	↓ Mg^{++} MDD; ↑ PCr in T3 responders
Forester *et al.*[20]	11 MDD 10 controls	70.7 ± 9.5 73.6 ± 6.3	4M : 7F 5M : 5F	Unmedicated	Gray and white matter	↓ White matter total NTP MDD

A summary of the ^{31}P MRS bioenergetic literature in subjects with major depressive disorder (MDD). PCr, phosphocreatine; β-NTP, β-nucleoside triphosphate. All metabolite comparisons of MDD are relative to normal (healthy) populations unless otherwise indicated. Arrows indicate increases (up) and decreases (down).

Table 2. Bipolar disorder and bioenergetics

References	Sample size	Age (mean ± SD) years	Sex	Medication status	Magnet/target	Metabolite
Kato *et al.*[23]	17 BPD	40.1 ± 10.8	8M : 9F	17 medicated	1.5 T; surface coil on frontal lobe	↓ pH; ↑ $[H^+]$
	17 control	39.1 ± 10.1	8M : 9F			
Kato *et al.*[24]	15 BP-II	43.1 ± 14.5	2M : 13F	12 medicated	1.5 T; surface coil on frontal lobe	↓ PCr in BP-II; all mood states
	14 BP-I	42.9 ± 9.6	6M : 8F	12 medicated		
	59 control	38.1 ± 12.6	27M : 32F			
Deicken *et al.*[25]	12 BPD	40.1 ± 8.3	10M : 2F	Unmedicated	2 T; MRSI temporal lobes	No differences
	14 control	39.8 ± 10.2	12M : 2F			
Murashita *et al.*[26]	19 BPD	46.3 ± 10.4	3M : 16F	18 medicated	1.5 T; surface coil occ. lobe; baseline and PS	↓ PCr after PS in Li^+ non-responders
	25 control	37.0 ± 14.0	12M : 13F			
Hamakawa *et al.*[27]	13 BPD	49.4 ± 12.1	7M : 6F	13 medicated	1.5 T; DRESS; basal ganglia	↓ pH; ↑ $[H^+]$
	10 control	43.2 ± 13.7	6M : 4F			
Shi *et al.*[28]	8 BPD	15.6 ± 1.0	3M : 5F	Unmedicated	3 T; MRSI; voxel located in anterior cingulate	↑ PCr under no medication; ↓ Pi under no medication and medication
	6 BPD	15.5 ± 0.8	4M : 2F	Medicated		
	24 control	15.7 ± 1.7	13M : 11F			
Sikoglu *et al.*[29]	8 BPD	15.5 ± 3.2	4M : 4F	8 medicated	4 T; MRSI-2-D; positioned AC-PC	↓ Global Pi; ↑ global PCr/Pi
	8 control	16.9 ± 2.0	6M : 2F			
Yuksel *et al.*[30]	23 BPD	27.5 ± 7.0	15M : 8F	Medicated	4 T; occ. surface coil: PS	BPD: ↓ ATP after PS
	22 control	28.5 ± 7.5	12M : 10F			Control: ↓ PCr after PS

A summary of the ^{31}P MRS bioenergetic literature in subjects with bipolar disorder (BPD). MRSI, magnetic resonance spectroscopic imaging; 2-D, two-dimensional; occ., occipital; PS, photic stimulation. All metabolite comparisons of BPD are relative to a normal control population unless otherwise indicated. Arrows indicate increases (up) and decreases (down).

to have played a role in the earlier observed reductions in PCr where unmedicated patients with bipolar disorder showed greater right frontal lobe asymmetry in PCr than the left, but no significant difference from controls overall.[25] Unmedicated adolescents with bipolar disorder also showed no difference from controls, whereas bipolar subjects on medication had lower PCr when normalized to the total phosphate signal.[28]

A recent 2-D MRSI study of children with bipolar disorder who were on medication did not show any difference between their clinical status (manic, depressed, or euthymic) and pH or PCr. Pi, however, was significantly lower in the children with bipolar disorder and the PCr/Pi ratio was also higher, although this effect was interpreted as likely due to medication use.[29]

Another way to assess bioenergetic function is with a brain activation paradigm, which yields results analogous to the energetic responses of muscle tissue during exercise.[32] Two studies have used this technique by employing photic stimulation and measuring energy metabolites pre- and post-stimulation in patients with bipolar disorder and in controls. The first study[26] looked at lithium responders and non-responders compared to controls in response to a flashing bright light stimulus. PCr was noted to be higher in patients with bipolar disorder as compared to controls, and PCr in Li^+-resistant patients was shown to be reduced more by photic stimulation than in Li^+-responders or in control subjects. A recent study employing this technique,[30] with the photic stimulation provided by a flashing stimulus operating at 8 Hz as compared to no photic stimulation, found differential changes in controls and bipolar subjects in total ATP, and in PCr levels and PCr/ATP. PCr was found to be reduced, as predicted, following stimulation in healthy controls but this was not the case for patients with bipolar disorder. Total ATP was found to be reduced in patients with bipolar disorder following the visual stimulus but not in normal controls.

Schizophrenia

A summary of results from ^{31}P MRS studies of bioenergetics in schizophrenia is presented in Table 3. Changes in bioenergetic molecules seen in schizophrenia patients appear to be highly dependent on localization and medication status. The first study of drug-free schizophrenic patients showed higher β-NTP and lower Pi when compared to normal controls in a voxel placed in the dorsolateral prefrontal cortex.[33] In follow-up studies performed in patients with chronic schizophrenia and mixed medication status, voxels placed in the bilateral temporal

Table 3. Schizophrenia and energetics

References	Sample size	Age (mean ± SD) years	Sex	Medication status	Magnet/target	Metabolite
Pettegrew *et al.*[33]	11 SCZ	24.4 ± 3.2	7M : 4F	Unmedicated	1.5 T; surface coil frontal lobe	↑ ATP; ↓ Pi
	10 control	24.1 ± 3.2	6M : 4F			
Calabrese *et al.*[34]	11 SCZ	39 ± 6	10M : 1F	9 medicated	2 T; 87 ml volume bilateral temporal lobe	↑ PCr/ATP on right vs. left compared to control
	9 control	35 ± 10	9M : 0F			
Deicken *et al.*[35]	20 SCZ	39.2 ± 5.8	20M : 0F	12 medicated	2 T; 2-D MRSI; bilateral frontal and parietal	↓ PCr frontal; ↓ Pi left frontal
	16 control	40.3 ± 11.0	16M : 0F			
Deicken *et al.*[36]	18 SCZ	39.4 ± 6.0	18M : 0F	13 medicated	2 T; 2-D MRSI; bilateral temporal	↑ PCr/ATP and ↑ PCr/Pi on right vs. left
	14 control	39.0 ± 5.3	14M : 0F			
Volz *et al.*[37]	50 SCZ	37.6 ± 11.2	31M : 19F	Medicated	1.5 T; ISIS; frontal	↑ PCr
	36 control	34.6 ± 11.9	20M : 16F			
Bluml *et al.*[38]	13 SCZ	34.3 ± 5.8	Not reported	11 medicated	Central volume	↑ PCr
	15 control	25.3 ± 4.7				
Jensen *et al.*[39]	15 SCZ	22.5 ± 3.4	13M : 2F	5 medicated; 10 naive; all first episode	4 T; MRSI	ACC; ↑ PCr; ↑ ATP
	15 control	22.1 ± 3.0	13M : 2F			
Smesny *et al.*[40]	31 SCZ	37.1 ± 11.4	15M : 16F	12 medicated; 12 naive; first episode	1.5 T; 2-D MRSI	Regional analysis ↓ PCr; ↓ Pi; ↓ ATP
	31 control	37.2 ± 11.3	15M : 16F			
Smesny *et al.*[41]	17 SCZ	39.8 ± 11.8	4M : 3F	Medication free then	1.5 T; 2-D MRSI	Haloperidol ↓ ATP; risperidone ↑ PCr; ↑ ATP
		38.5 ± 14.4	4M : 6F	Tx haloperidol Tx risperidone		
Du *et al.*[42]	26 SCZ	34.5 ± 8.4	13M : 13F	26 medicated	4 T; Magnetization transfer; frontal	↓ CK flux
	26 control	31.9 ± 8.9	14M : 12F			

A summary of the ^{31}P MRS bioenergetic literature in subjects with schizophrenia (SCZ). ACC, anterior cingulate cortex; 2-D, two-dimensional. All metabolite comparisons of schizophrenia are relative to a normal control population unless otherwise indicated. Arrows indicate increases (up) and decreases (down).

lobes showed reduced mole percent PCr compared to normal adults[35] whereas no differences in parietal cortex energetic metabolites were observed. A study that explicitly compared patients with schizophrenia on medication to those who were not on neuroleptic medication and normal controls found that PCr mol% and ATP mol% were significantly increased only in patients who were on neuroleptic medication, whereas those who were medication free resembled controls, leading the authors to suggest that neuroleptic medication was decreasing the metabolic demand for high-energy phosphate.[37] A similar finding of increased PCr mol% with medicated patients with schizophrenia was made in the parietal cortex[38] although another study showed no change.[35]

Results in the temporal lobe have generally focused on imbalances in energetic compounds between the right and left hemispheres, with energetic compounds, PCr[36] and PCr/Pi and PCr/β-NTP,[34,36] generally found to be higher in the right hemisphere compared to the left. In a study of drug-naive first-episode patients, however, higher left temporal PCr was observed when compared with a matched control sample, whereas no difference was observed in the right temporal region.[41]

All of the above studies were performed on magnets with a field strength of 1.5–2 T. A more recent study of the anterior cingulate cortex and left thalamus, cerebellum, and hippocampus performed at 4 T found, in patients who were largely neuroleptic free, higher levels of PCr, βNTP, and Pi in the anterior cingulate but no differences in other brain regions when compared to a normal control population.[39] A second study at 4 T using 3-D MRSI and segmenting GM from WM found that β-NTP was decreased in GM whereas β-NTP was increased in WM.

In a more recent study of bioenergetics at 4 T employing 2-D MRSI using antipsychotic-naive patients, evidence emerged of a reduction of PCr and Pi when compared to controls in a large range of brain areas including the frontal cortex and medial temporal lobe.[40] Another recent study examining the CK equilibrium rate constant[42] showed that the rate constant in the frontal lobe was reduced by 22% in patients with schizophrenia compared to controls, with an accompanying decrease in pH corresponding to a 7% increase in [H^+]. However, no differences were seen in the overall levels of energetic metabolites. Increasing H^+ concentrations should favor the formation

of ATP from PCr, yet the equilibrium suggests a reduction in the forward reaction rate of generation of ATP from PCr.

Summary

One question that emerges from these studies is why alterations are seen sometimes only in PCr and other times in NTP, since both reflect available high-energy phosphate levels. The difference between them may reflect the differing roles wherein PCr acts as a temporal and sometimes spatial buffer of high-energy phosphate for ATP, which is then utilized to drive cellular reactions. Perhaps the answer may also be found in the differing enzymatic activities of the isozymes of CK. These isozymes have different distributions in GM and WM, which may affect the role of PCr in acting as a spatial buffer in GM versus WM. The brain, particularly GM, is one of the most metabolically active organs in the body, consuming approximately 20% of the total energy of the body while comprising less than 2% of the body weight.[4,43] In addition, while levels of ATP, ADP, AMP, PCr, and Cr are similar for GM and WM, energy utilization based on studies of glucose utilization is two to four times higher in GM than in WM,[4,44,45] while blood flow is four to five times higher in GM.[46] This means that most of the brain's metabolic activity and highest demand for ATP occurs in GM.

Therefore, based on the differing metabolic needs in GM versus WM, it may be that CK plays different roles in the two tissue types, with a PCr shuttle operating between mitochondria and the cytoplasm in GM similar to the heart and muscle, whereas WM acts similar to a tissue wherein the energetic needs are much lower. In tissues with high energy needs, PCr acts as a shuttle[47] to rapidly transport high-energy phosphate from the mitochondria to the cytoplasm to regenerate ATP. This is mediated by two different isoforms of CK: mitochondrial creatine kinase (Mi-CK), located in the mitochondria, and brain creatine kinase (BB-CK), located in the cytosol.[48] Mi-CK catalyzes the forward reaction,[49] transferring a high-energy phosphate from ATP to Cr yielding ADP and PCr, which diffuses to the cytoplasm. BB-CK catalyzes the reverse reaction in the cytosol from PCr and ADP to Cr and ATP. The much lower Mi-CK levels in WM compared to GM suggest that ATP diffuses from the mitochondria to the cytosol without generating the intermediary PCr.[48] This would lead to the conclusion that when a voxel is placed in a region containing greater amounts of WM, the energetic status of the tissue will be indicated by changing levels of ATP, whereas energetic changes in regions with greater amounts of GM will likely manifest as changes in PCr.

Membrane Metabolism and ^{31}P MRS

Depression and Bipolar Illness

A summary of results from ^{31}P MRS studies of phospholipids in unipolar and bipolar depression is presented in Table 4. Studies of patients with unipolar major depression that examined phospholipid metabolites have in general shown no change in either PME or PDE in examinations of the frontal region and the basal ganglia.[15,16] However, studies of patients with bipolar depression do show changes in membrane phospholipids in specific disease states (manic, euthymic, or depressed). In particular, two early studies of patients with bipolar illness demonstrated a reduction in PME in patients in the euthymic state that was not observed in either the manic state[50] or the depressed state.[15] Again, the medication status of these patients may be an important factor in these studies since they involved

Table 4. Depression and bipolar illness and phospholipid metabolism

References	Sample size	Age (mean ± SD) years	Sex	Medication status	Magnet/target	Metabolite
Kato *et al.*[50]	11 BPD	40.8 ± 11.0	7M : 4F	6 medicated	1.5 T; surface coil; DRESS; frontal	↑ PME in manic state
	9 control	39.8 ± 10.9	5M : 4F			
Kato *et al.*[15]	12 MDD	35.3 ± 12.1	5M : 7F	8 medicated	1.5 T; surface coil; DRESS; frontal	↓ PME in euthymic bipolar
	10 BPD	42.0 ± 8.6	4M : 6F	4 medicated		
Moore *et al.*[16]	35 MDD	37.2 ± 8.5	16M : 19F	Unmedicated	1.5 T; basal ganglia	No differences
	18 control	38.2 ± 9.9	9M : 9F			
Deicken *et al.*[51]	12 BPD	40.1 ± 8.3	10M : 2F	11 medicated	2 T; 2-D MRSI; bilateral temporal	↓ PME; left and right temporal
	14 control	39.8 ± 10.2	12M : 2F			
Deicken *et al.*[25]	12 BPD	40.1 ± 8.3	10M : 2F	Unmedicated	2 T; 2-D MRSI frontal lobes	↓ PME; ↑ PDE left and right frontal
	14 control	39.8 ± 10.2	12M : 2F			
Shi *et al.*[28]	8 BPD	15.6 ± 1.0	3M : 5F	Unmedicated	3 T; MRSI; voxel located in anterior cingulate	No differences
	6 BPD	15.5 ± 0.8	4M : 2F	Medicated		
	24 control	15.7 ± 1.7	13M : 11F	Control		

A summary of the ^{31}P MRS phospholipid literature in subjects with bipolar depression and major depression. DRESS, depth resolved surface coil spectroscopy; PME, phosphomonoesters; PDE, phosphodiesters. All metabolite comparisons of the affective disorder are relative to a normal control population, unless otherwise indicated. Arrows indicate increases (up) and decreases (down).

euthymic, medicated patients often taking lithium. Studies performed with euthymic patients that were medication free for 1 week demonstrated lower PME[25,51] bilaterally in the temporal and frontal lobes, and higher PDE in the frontal lobes bilaterally.[25] More recent studies of bipolar illness have not noted significant differences in phospholipids in the children and adolescents involved in these studies.[28]

Schizophrenia

A summary of results from ^{31}P MRS studies of phospholipids in schizophrenia is presented in Table 5. Membrane metabolism, measured with ^{31}P MRS, has been shown to be highly variable in schizophrenia, with both increases and decreases in PME and PDE being noted, making it difficult to characterize systematically what drives the differences and what these differences might mean. It would appear that the chronicity or duration of illness, the status of medications,[59] the region of tissue being sampled,[39,60] and the composition of GM and WM in the voxel or region of interest[61] may play important roles.

The first in vivo study of phospholipid metabolism in schizophrenia involved 11 well-characterized drug-naive, first-episode patients and found decreased PME and increased PDE from voxels placed bilaterally in the dorsoprefrontal cortex.[33]

Table 5. Schizophrenia and phospholipids

References	Sample size	Age (mean ± SD) years	Sex	Medication status	Magnet/target	Metabolite
Pettegrew *et al.*[33]	11 SCZ	24.4 ± 3.2	7M : 4F	First episode; drug naive	1.5 T; surface coil; frontal lobe	↓ PME; ↑ PDE
	10 control	24.1 ± 3.2	6M : 4F			
Williamson *et al.*[52]	10 SCZ	38.7 ± 6.0	9M : 1F	Medicated	2 T; surface coil; frontal lobe	↓ PME
	7 Control	Matched	Matched			
Stanley *et al.*[53]	19 SCZ	32 ± 10	No info	Medicated	2 T; surface coil; frontal lobe	↓ PME all; ↑ PDE newly diagnosed
	18 control	31 ± 10	18M : 0F			
Deicken *et al.*[35]	20 SCZ	39.2 ± 5.8	20M : 0F	12 medicated	2 T; 2-D MRSI; bilateral frontal and parietal	↑ PDE frontal only
	16 control	40.3 ± 11.0	16M : 0F			
Stanley *et al.*[54]	29 SCZ	N/A	25M : 4F	Mixture	2 T; surface coil	↓ PME all; ↑ PDE in first episode no medication
	17 control	31 ± 9	17M : 4F		Frontal lobe	
Volz *et al.*[37]	13 SCZ	29.6 ± 7.4	10M : 4F	Medicated	1.5 T; ISIS; bilateral DLPFC	↓ PDE
	14 control	32.9 ± 8.1	7M : 4F			
Volz *et al.*[55]	50 SCZ	37.6 ± 11.2	31M : 19F	Medicated	1.5 T; ISIS; bilateral DLPFC	↓ PDE
	36 control	34.6 ± 11.9	20M : 16F			
Bluml *et al.*[38]	13 SCZ	34.3 ± 5.8	Not reported	11 medicated	Central volume	↑ GPCho; ↑ GPEtn
	15 control	25.3 ± 4.7				
Fukuzako *et al.*[56]	17 SCZ	23.1	10M : 7F	First episode; drug naive	2 T; 2-D MRSI	↓ PME; ↑ PDE
	17 control	22.5	Not reported			
Jensen *et al.*[39]	15 SCZ	22.5 ± 3.4	13M : 2F	12 medicated; 12 naive; first episode	4 T; MRSI	↑ GPCho in ACC in naive; first episode
	15 control	22.1 ± 3.0	13M : 2F			
Miller *et al.*[57]	13 SCZ	Not reported	12M : 1F	T_0: 6 medicated; T_{30}: 10 medicated	4 T; MRSI 3-D; anterior cingulate; left thalamus	↑ GPCho in ACC at Time 0;
	13 control		12M : 1F			↓ GPEth at 30 months
Miller *et al.*[58]	16 SCZ	22 ± 4	14M : 2F	T_{10}: 12 medicated; T_{52}: 11 medicated	4 T; MRSI 3-D; ACC, PCC, HPC, THL, STG, PFC	T_{10}: ↑ GPCho in ACC; T_{52}: ↑ GPCho PCC, STG, ↑ GPEtn HPC, ↓ GPEtn THL, PFC compared to T_{10}
	16 control	25 ± 6	14M : 2F			
Smesny *et al.*[41]	17 SCZ	39.8 ± 11.8	4M : 3F	Baseline scan; 7 treated haldoperidol; 10 risperidone	1.5 T MRSI 2-D	Haloperidol ↓ PME; ↓ PDE Risperidone ↑ PDE
		38.5 ± 14.4	4M : 6F			

A summary of the ^{31}P MRS phospholipid literature in subjects with schizophrenia (SCZ). T_0, time of diagnosis; T_{30}, 30 months after diagnosis; T_{10}, 10 months following diagnosis; T_{52}, 52 months after diagnosis; ACC, anterior cingulate cortex; PCC, posterior cingulate cortex; HPC, hippocampus; THL, thalamus; STG, superior temporal gyrus; PFC, prefrontal cortex. All metabolite comparisons of schizophrenia are relative to control populations unless otherwise indicated. Arrows indicate increases (up) and decreases (down).

A contemporaneous small study of medicated patients showed that the medication status or duration of illness caused some subtle differences, with PME being decreased but PDE showing no change.[52] This difference was further clarified in a follow-up study from the same group analyzing a larger cohort showing that, while PME was still reduced in the patients with schizophrenia, PDE was also significantly higher in newly diagnosed but medicated patients, as compared to chronic patients and controls.[53] These changes are seen quite consistently in first-episode, drug-naive patients.[39,54,56] In patients with chronic schizophrenia who have been taking medication consistently, the results are much more variable, with studies reporting both increases[35] and decreases[37,55] in PDE levels.

Several methodological and study design changes have been explored to tackle the sources of variance seen in these studies and attempt to find a context for these early results. A study using proton-decoupling techniques to resolve the PDE resonance into independently measurable GPCho and GPEtn resonances found that both of these PDEs were elevated in the parietal cortex of a mixed chronic and first-episode cohort of patients with schizophrenia, as compared to normal controls.[38] No differences in PMEs were observed in these subjects. A repeat study with MRS voxels placed bilaterally in the temporal lobes showed increased PDE and decreased PME in 17 first-episode patients[56] compared to 19 healthy controls. A follow-up study of 13 first-episode patients before and after treatment with haloperidol showed that while PME was decreased and PDE increased compared to controls, treatment with haloperidol normalized the PDE levels. Further support for first-episode differences from chronic schizophrenia was obtained from studies of children at high risk for developing schizophrenia. In these subjects, with voxel placement in the frontal cortex, reduced PME was seen in children and adolescent children of parents who had schizophrenia,[62] and increased PDE was also seen in a cohort of 18 children at high risk of developing schizophrenia.[63]

Increases in PDE have also been observed in studies of medicated[64] and unmedicated[65] subjects with schizophrenia with voxels placed in the temporal cortex. When haloperidol is given to unmedicated subjects with schizophrenia, PDE measured in the temporal cortex is observed to decrease.[65]

An attempt to quantify the temporal and spatial dynamics of phospholipid changes in schizophrenia was recently undertaken in a cohort of patients with recent diagnosis who were followed for an extended period.[58] The pattern that emerged from the data, especially in the frontal regions, is that PDE is increased in first-episode patients compared to control subjects, but is not different from controls in patients who have been treated for a significant period of time, particularly those treated with first-generation antipsychotics such as haloperidol. It remains unclear, however, whether both constituents of the PDE peak are involved in these changes. A systematic, repeated measures study demonstrated the same effect in the same patients[57] scanned 30 months apart: GPCho was higher compared to that in controls in the anterior cingulate but GPEtn was not significantly different. At 30 months, GPEtn was significantly lower in the left thalamus.

A further examination of PDE dynamics was made in a study of 16 first-episode patients with schizophrenia and 16 matched controls at a baseline assessment and 39 months later using single voxels placed in the prefrontal cortex, anterior cingulate, posterior cingulate, superior temporal gyrus, temporal pole, hippocampus, and thalamus. This study confirmed observations of increased GPCho in the anterior cingulate of patients at baseline, which then decreased at 39 months. In the posterior cingulate, GPCho level was not different from that in normal controls at baseline but increased at 39 months. Time and spatial dynamics were also evident, with both GPCho and GPEth increased in the superior temporal gyrus at 39 months. In the thalamus GPEth was markedly reduced in schizophrenia patients at 39 months compared to baseline in the patients and in the controls.[58]

A study of phospholipid metabolites that controlled for partial volume effects and tissue type was recently published as well. In chronic schizophrenia, frontal cortex and cerebellar GPCho were reduced, whereas PEth was reduced in the frontal cortex and PCho was reduced in the lateral basal ganglia.[41]

A number of factors make these studies difficult to interpret including small sample sizes, the spatial placement of voxels, and the size of the voxels including partial volume effects from tissues not targeted. It does appear from these studies that tissue type, chronicity of illness, and the region targeted all have an impact on the measured phospholipids.

Membrane Synthesis and the Role of Phospholipase A2

The data cited above indicate that membrane metabolism plays a significant role in pathologies related to schizophrenia. However, the meaning of the metabolic changes is not obvious without reference to the metabolic pathways themselves. Phosphatidylcholine is synthesized from PCho directly via the CDP-choline pathway (half of the Kennedy pathway).[66] It can also be generated from phosphatidylethanolamine via phosphatidylethanolamine *N*-methyltransferase (PEMT).[67,68] In an analogous manner, phosphatidylethanolamine can be synthesized from PEtn via the CDP-ethanolamine pathway (the other half of the Kennedy pathway)[66]; however, it cannot be directly synthesized from PCho since PEMT only interacts with the phosphatidylethanolamine substrate (Figure 4).

Phosphatidylcholine and phosphatidylethanolamine are both deacylated by phospholipase A2 (PLA2)[2] into lysophosphatidylcholine and lysophosphatidylethanolamine, which are subsequently transformed into GPCho and GPEtn.[69] Membranes are maintained in a homeostatic equilibrium between synthesis and degradation by the action of a calcium-independent phospholipase A2 (iPLA2).[2,70–73] Increasing membrane precursor availability, either by adding exogenous precursor or by increasing the efficiency of the CDP-PCho citydyltransferase, has been noted to increase the quantity of GPCho or GPEtn in cell cultures[70] and in healthy tissue.[2,3] Characteristics of membrane turnover as mediated by calcium iPLA2, can be estimated by measuring the relative levels of PME and PDE in the brain.[74]

Membrane phospholipids also serve as an important source of second messengers that function to mediate the inflammatory responses to proinflammatory cytokines and

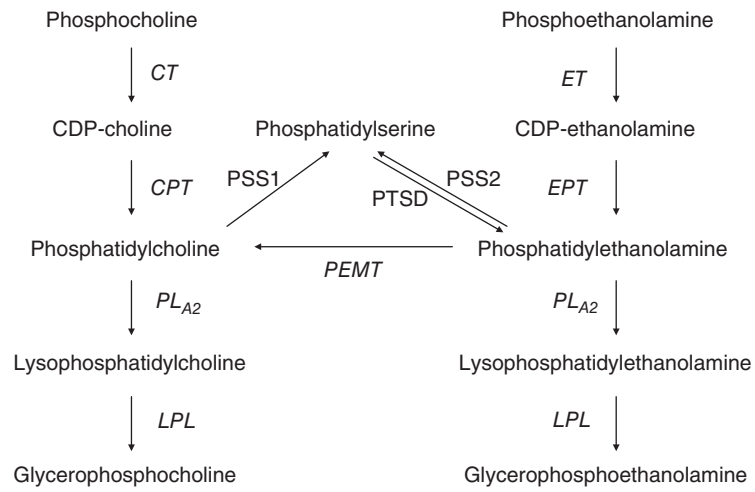

Figure 4. Biosynthetic pathways of phosphatidylcholine and phosphatidylethanolamine (Kennedy pathways). CT, CTP: phosphocholine cytidylyltransferase; ET, CTP: phosphoethanolamine cytidylyltransferase; CPT, CDP-choline: 1,2-diacylglycerol cholinephosphotransferase; PEMT, phosphatidylethanolamine *N*-methyltransferase; PTSD, phosphatidylserine decarboxylase; PSS, phsophatidylserine syntase; PLA2, phospholipase A2; LPL, lysophospholipase

other immune signaling. In contrast to the iPLA2s, cytosolic phospholipase A2s (cPLA2) and secretory phospholipase A2s (sPLA2) release arachidonic acid during the process of breaking down cell membranes.[75] Arachidonic acid, an eicosanoid and leukotriene precursor,[76] acts as an intracellular second messenger of immune activation in the brain. The activation and gene expression of cPLA2 are stimulated by IL-1β and TNF-α,[77] especially in the presence of calcium.[78,79] This results in intracellular arachidonic acid release through second messengers, thereby altering synaptic proteins[77] while also inducing Na^+ and Ca^{++} entry into the cell, resulting in mitochondria-mediated apoptosis.[80] ^{31}P MRS can detect these immune activation signals by quantifying changes in the PME and PDE pools in tissue.[81,82]

In summary, it is likely that PMEs, when they increase with PDEs, indicate normal reconditioning of cell membranes. However, when PDEs vary inversely from PMEs, and are elevated, they may signify a central inflammatory state. Such is the case seen in many studies of patients with schizophrenia.[83–85]

Conclusion

^{31}P MRS can provide a wealth of biochemical information on high-energy phosphates, membrane precursors, and metabolites that are essential for cellular survival and impact the overall state of health of the cell. Fusing biochemical knowledge with the exquisite physics of ^{31}P MRS can yield unique insight into the energetic and homeostatic nature of the cells of the brain.

Biographical Sketches

David G. Harper, PhD is an assistant professor of psychology in the Department of Psychiatry at Harvard Medical School and an associate research psychologist at McLean Hospital where he serves as Associate Director for Research in the Division of Geriatric Psychiatry. He received his BS, MS, and PhD degrees in Biology and Psychology from Tufts University.

J. Eric Jensen, PhD is an assistant professor of psychiatry at Harvard Medical School and a biophysicist at McLean Hospital. Dr. Jensen joined the McLean Imaging Center in 2002 focusing on improved proton/phosphorus spectroscopic imaging/quantification methods in the assessment of brain neurotransmission and bioenergetics/phospholipid metabolism in psychiatric disorders.

Perry F. Renshaw received his MD and PhD (Biophysics) degrees from the University of Pennsylvania. Following a residency in general psychiatry at the Massachusetts General Hospital, he served as Director of the McLean Hospital Brain Imaging Center and as a professor of psychiatry at Harvard Medical School. In 2008, Dr. Renshaw accepted a position as a USTAR Professor of Psychiatry at the University of Utah.

References

1. J. E. Vance, *J. Lipid Res.*, 2008, **49**, 1377.
2. I. Baburina and S. Jackowski, *J. Biol. Chem.*, 1999, **274**, 9400.
3. S. M. Babb, L. L. Wald, B. M. Cohen, R. A. Villafuerte, S. A. Gruber, D. A. Yurgelun-Todd, and P. F. Renshaw, *Psychopharmacology (Berl)*, 2002, **161**, 248.
4. M. Erecinska and I. A. Silver, *J. Cereb. Blood Flow Metab.*, 1989, **9**, 2.
5. T. Wallimann, M. Wyss, D. Brdiczka, K. Nicolay, and H. M. Eppenberger, *Biochem. J.*, 1992, **281**, 21.
6. D. L. Friedman and R. Roberts, *J. Comp. Neurol.*, 1994, **343**, 500.
7. G. J. Kemp, D. N. Manners, J. F. Clark, M. E. Bastin, and G. K. Radda, *Mol. Cell. Biochem.*, 1998, **184**, 249.
8. B. Chance, J. S.Leigh Jr,, J. Kent, K. McCully, S. Nioka, B. J. Clark, J. M. Maris, and T. Graham, *Proc. Natl. Acad. Sci. U. S. A.*, 1986, **83**, 9458.
9. S. Bose, S. French, F. J. Evans, F. Joubert, and R. S. Balaban, *J. Biol. Chem.*, 2003, **278**, 39155.
10. D. Phillips, A. M. Aponte, S. A. French, D. J. Chess, and R. S. Balaban, *Biochemistry*, 2009, **48**, 7140.
11. J. P. Schmitz, J. A. Jeneson, J. W. van Oorschot, J. J. Prompers, K. Nicolay, P. A. Hilbers, and N. A. van Riel, *PLoS One*, 2012, **7**, e34118.
12. O. A. Petroff, J. W. Prichard, K. L. Behar, J. R. Alger, J. A.den Hollander, and R. G. Shulman, *Neurology*, 1985, **35**, 781.

13. S. Iotti, C. Frassineti, L. Alderighi, A. Sabatini, A. Vacca, and B. Barbiroli, *NMR Biomed.*, 1996, **9**, 24.
14. E. M. Golding, W. E.Teague Jr,, and G. P. Dobson, *J. Exp. Biol.*, 1995, **198**, 1775.
15. T. Kato, S. Takahashi, T. Shioiri, and T. Inubushi, *J. Affect. Disord.*, 1992, **26**, 223.
16. C. M. Moore, J. D. Christensen, B. Lafer, M. Fava, and P. F. Renshaw, *Am. J. Psychiatry*, 1997, **154**, 116.
17. H. P. Volz, R. Rzanny, S. Riehemann, S. May, H. Hegewald, B. Preussler, G. Hubner, W. A. Kaiser, and H. Sauer, *Eur. Arch. Psychiatry Clin. Neurosci.*, 1998, **248**, 289.
18. P. F. Renshaw, A. M. Parow, F. Hirashima, Y. Ke, C. M. Moore, B. Frederick, M. Fava, J. Hennen, and B. M. Cohen, *Am. J. Psychiatry*, 2001, **158**, 2048.
19. D. V. Iosifescu, N. R. Bolo, A. A. Nierenberg, J. E. Jensen, M. Fava, and P. F. Renshaw, *Biol. Psychiatry*, 2008, **63**, 1127.
20. B. P. Forester, D. G. Harper, J. E. Jensen, C. Ravichandran, B. Jordan, P. F. Renshaw, and B. M. Cohen, *Int. J. Geriatr. Psychiatry*, 2009, **24**, 788.
21. Association AP, Diagnostic and Statistical Manual of Mental Disorders, American Psychiatric Press: Washington, DC, 1987.
22. M. Hamilton, *Br. J. Soc. Clin. Psychol.*, 1967, **6**, 278.
23. T. Kato, S. Takahashi, T. Shioiri, and T. Inubushi, *J. Affect. Disord.*, 1993, **27**, 53.
24. T. Kato, S. Takahashi, T. Shioiri, J. Murashita, H. Hamakawa, and T. Inubushi, *J. Affect. Disord.*, 1994, **31**, 125.
25. R. F. Deicken, G. Fein, and M. W. Weiner, *Am. J. Psychiatry*, 1995, **152**, 915.
26. J. Murashita, T. Kato, T. Shioiri, T. Inubushi, and N. Kato, *Psychol. Med.*, 2000, **30**, 107.
27. H. Hamakawa, J. Murashita, N. Yamada, T. Inubushi, N. Kato, and T. Kato, *Psychiatry Clin. Neurosci.*, 2004, **58**, 82.
28. X. F. Shi, D. G. Kondo, Y. H. Sung, T. L. Hellem, K. K. Fiedler, E. K. Jeong, R. S. Huber, and P. F. Renshaw, *Bipolar Disord.*, 2012, **14**, 607.
29. E. M. Sikoglu, J. E. Jensen, G. Vitaliano, A. A. Liso Navarro, P. F. Renshaw, J. A. Frazier, and C. M. Moore, *PLoS One*, 2013, **8**, e54536.
30. C. Yuksel, F. Du, C. Ravichandran, J. R. Goldbach, T. Thida, P. Lin, B. Dora, J. Gelda, L. O'Connor, S. Sehovic, S. Gruber, D. Ongur, and B. M. Cohen, *Mol. Psychiatry*, 2015, **20**, 1079.
31. T. Kato, T. Shioiri, J. Murashita, H. Hamakawa, Y. Takahashi, T. Inubushi, and S. Takahashi, *Psychol. Med.*, 1995, **25**, 557.
32. B. Chance, *Ann. N. Y. Acad. Sci.*, 1984, **428**, 318.
33. J. W. Pettegrew, M. S. Keshavan, K. Panchalingam, S. Strychor, D. B. Kaplan, M. G. Tretta, and M. Allen, *Arch. Gen. Psychiatry*, 1991, **48**, 563.
34. G. Calabrese, R. F. Deicken, G. Fein, E. L. Merrin, F. Schoenfeld, and M. W. Weiner, *Biol. Psychiatry*, 1992, **32**, 26.
35. R. F. Deicken, G. Calabrese, E. L. Merrin, D. J. Meyerhoff, W. P. Dillon, M. W. Weiner, and G. Gein, *Biol. Psychiatry*, 1994, **36**, 503.
36. R. F. Deicken, G. Calabrese, E. L. Merrin, S. Vinogradov, G. Fein, and M. W. Weiner, *Biol. Psychiatry*, 1995, **38**, 279.
37. H. P. Volz, R. Rzanny, G. Rossger, G. Hubner, L. Kreitschmann-Andermahr, W. A. Kaiser, and H. Sauer, *Biol. Psychiatry*, 1998, **44**, 399.
38. S. Bluml, J. Tan, K. Harris, N. Adatia, A. Karme, T. Sproull, and B. Ross, *J. Comput. Assist. Tomogr.*, 1999, **23**, 272.
39. J. E. Jensen, J. Miller, P. C. Williamson, R. W. Neufield, R. S. Menon, A. Malla, R. Manchanda, B. Schaefer, M. Densmore, and D. J. Drost, *Br. J. Psychiatry*, 2004, **184**, 409.
40. S. Smesny, T. Rosburg, I. Nenadic, K. P. Fenk, S. Kunstmann, R. Rzanny, H. P. Volz, and H. Sauer, *Neuroimage*, 2007, **35**, 729.
41. S. Smesny, K. Langbein, R. Rzanny, A. Gussew, H. P. Burmeister, J. R. Reichbach, and H. Sauer, *Schizophr. Res.*, 2012, **138**, 164.
42. F. Du, A. J. Cooper, T. Thida, S. Sehovic, S. E. Lukas, B. M. Cohen, X. Zhang, and D. Ongur, *JAMA Psychiatry*, 2014, **71**, 19.
43. D. D. Clarke and L. Sokoloff, in Basic Neurochemistry, ed G. Siegal, Lippincott, Williams & Wilkins: Philadelphia, 1999, 638.
44. L. Sokoloff, M. Reivich, C. Kennedy, M. H. Des Rosiers, C. S. Patlak, K. D. Pettigrew, O. Sakurada, and M. Shinohara, *J. Neurochem.*, 1977, **28**, 897.
45. X. H. Zhu, H. Qiao, F. Du, Q. Xiong, X. Liu, X. Zhang, K. Ugurbil, and W. Chen, *Neuroimage*, 2012, **60**, 2107.
46. D. Clark and L. Sokoloff, in Basic Neurochemistry: Molecular, Cellular, and Medical Aspects, 6th edn, eds G. Siegal, B. Agranoff, R. Albers, S. Fisher and M. Uhler, Raven Press: New York, 1999.
47. R. A. Meyer, H. L. Sweeney, and M. J. Kushmerick, *Am. J. Physiol.*, 1984, **246**, C365.
48. D. Holtzman, J. M. Benzecry, and T. Kekelidze, in Creatine Kinase and Brain Energy Metabolism: Function and Disease, eds T. Kekelidze and D. Holtzman, IOS Press: Amsterdam, The Netherlands, 2003, 25.
49. F. A.van Dorsten, R. Furter, M. Bijkerk, T. Wallimann, and K. Nicolay, *Biochim. Biophys. Acta*, 1996, **1274**, 59.
50. T. Kato, T. Shioiri, S. Takahashi, and T. Inubushi, *J. Affect. Disord.*, 1991, **22**, 185.
51. R. F. Deicken, M. W. Weiner, and G. Fein, *J. Affect. Disord.*, 1995, **33**, 195.
52. P. Williamson, D. Drost, J. Stanley, T. Carr, S. Morrison, and H. Merskey, *Arch. Gen. Psychiatry*, 1991, **48**, 578.
53. J. A. Stanley, P. C. Williamson, D. J. Drost, T. J. Carr, R. J. Rylett, S. Morrison-Stewart, and R. T. Thompson, *Schizophr. Res.*, 1994, **13**, 209.
54. J. A. Stanley, P. C. Williamson, D. J. Drost, T. J. Carr, R. J. Rylett, A. Malla, and R. T. Thompson, *Arch. Gen. Psychiatry*, 1995, **52**, 399.
55. H. P. Volz, R. Rzanny, S. May, H. Hegewald, B. Preussler, M. Hajek, W. A. Kaiser, and H. Sauer, *Biol. Psychiatry*, 1997, **41**, 644.
56. H. Fukuzako, T. Fukuzako, T. Hashiguchi, S. Kodama, M. Takigawa, and T. Fujimoto, *Am. J. Psychiatry*, 1999, **156**, 1205.
57. J. Miller, P. Williamson, J. E. Jensen, R. Manchanda, R. Menon, R. Neufeld, N. Rajakumar, W. Pavlosky, M. Desnmore, B. Schaefer, and D. J. Drost, *Psychiatry Res.*, 2009, **173**, 155.
58. J. Miller, D. J. Drost, E. Jensen, R. Manchanda, S. Northcott, R. W. Neufeld, R. Menon, N. Rajakumar, W. Pavlosky, M. Desnmore, B. Schaefer, and P. Williamson, *Psychiatry Res.*, 2012, **201**, 25.
59. M. S. Keshavan, J. A. Stanley, and J. W. Pettegrew, *Biol. Psychiatry*, 2000, **48**, 369.
60. J. A. Stanley, J. W. Pettegrew, and M. S. Keshavan, *Biol. Psychiatry*, 2000, **48**, 357.
61. J. J. Potwarka, D. J. Drost, P. C. Williamson, T. Carr, G. Canaran, W. J. Rylett, and R. W. Neufeld, *Biol. Psychiatry*, 1999, **45**, 687.
62. M. S. Keshavan, J. A. Stanley, D. M. Montrose, N. J. Minshew, and J. W. Pettegrew, *Mol. Psychiatry*, 2003, **8**, 316.
63. R. Rzanny, S. Klemm, J. R. Reichenbach, S. O. Pfleiderer, B. Schmidt, H. P. Volz, B. Blanz, and W. A. Kaiser, *Eur. Radiol.*, 2003, **13**, 763.
64. T. Fujimoto, T. Nakano, T. Takano, Y. Hokazono, T. Asakura, and T. Tsuji, *Acta Psychiatr. Scand.*, 1992, **86**, 455.
65. H. Fukuzako, T. Fukuzako, S. Kodama, T. Hashiguchi, M. Takigawa, and T. Fujimoto, *Neuropsychopharmacology*, 1999, **21**, 542.
66. E. P. Kennedy and S. B. Weiss, *J. Biol. Chem.*, 1956, **222**, 193.
67. J. Bremer, P. H. Figard, and D. M. Greenberg, *Biochim. Biophys. Acta*, 1960, **43**, 477.
68. J. K. Blusztajn, S. H. Zeisel, and R. J. Wurtman, *Brain Res.*, 1979, **179**, 319.
69. S. C. Morash, H. W. Cook, and M. W. Spence, *Biochim. Biophys. Acta*, 1989, **1004**, 221.

70. S. C. Morash, H. W. Cook, and M. W. Spence, *Biochim. Biophys. Acta*, 1988, **961**, 194.
71. M. V. Winstead, J. Balsinde, and E. A. Dennis, *Biochim. Biophys. Acta*, 2000, **1488**, 28.
72. J. Balsinde and M. A. Balboa, *Cell. Signal.*, 2005, **17**, 1052.
73. S. E. Barbour, A. Kapur, and C. L. Deal, *Biochim. Biophys. Acta*, 1999, **1439**, 77.
74. D. G. Harper, J. E. Jensen, C. Ravichandran, Y. Sivrioglu, M. Silveri, D. V. Iosifescu, P. F. Renshaw, and B. P. Forester, *Am. J. Geriatr. Psychiatry*, 2014, **22**, 499.
75. E. A. Dennis, J. Cao, Y. H. Hsu, V. Magrioti, and G. Kokotos, *Chem. Rev.*, 2011, **111**, 6130.
76. M. Murakami and I. Kudo, *J. Biochem.*, 2002, **131**, 285.
77. J. S. Rao, M. Kellom, H. W. Kim, S. I. Rapoport, and E. A. Reese, *Neurochem. Res.*, 2012, **37**, 903.
78. W. G. Hoeck, C. S. Ramesha, D. J. Chang, N. Fan, and R. A. Heller, *Proc. Natl. Acad. Sci. U. S. A.*, 1993, **90**, 4475.
79. O. J. Jupp, P. Vandenabeele, and D. J. MacEwan, *Biochem. J.*, 2003, **374**, 453.
80. K. M. Fang, W. L. Chang, S. M. Wang, M. J. Su, and M. L. Wu, *J. Neurochem.*, 2008, **104**, 1177.
81. I. Ringel, S. Lecht, M. Sterin, P. I. Lelkes, and P. Lazarovici, *Endothelium*, 2008, **15**, 299.
82. K. Glunde, E. Ackerstaff, N. Mori, M. A. Jacobs, and Z. M. Bhujwalla, *Mol. Pharm.*, 2006, **3**, 496.
83. W. F. Gattaz, M. Kollisch, T. Thuren, J. A. Virtanen, and P. K. Kinnunen, *Biol. Psychiatry*, 1987, **22**, 421.
84. W. F. Gattaz, C. V. Hubner, T. J. Nevalainen, T. Thuren, and P. K. Kinnunen, *Biol. Psychiatry*, 1990, **28**, 495.
85. M. H. Law, R. G. Cotton, and G. E. Berger, *Mol. Psychiatry*, 2006, **11**, 547.